

JAMES R. DOWNEY\*  
JOHN H. ERKKILAAir Force Institute of Technology  
Wright-Patterson Air Force Base, OhioABSTRACT

A new time-independent numerical method is used to determine the late-time electromagnetic pulse (EMP) resulting from a surface nuclear burst. Completely arbitrary source terms are employed and the non-linear dependence of the air chemistry and air conductivity parameters on the electric field strength is incorporated into the solutions. Comparisons are made with previous analytic expressions. In addition, a parametric study is presented.

INTRODUCTION

Longmire and Gilbert (Ref 1) developed an analytic model describing the EMP from a surface nuclear explosion for times in which the quasi-static approximation is valid. In this model, the radial electric fields are taken to be zero everywhere. For specific functional forms of the Compton current and the air conductivity, they find the following expression for the polar electric field:

$$E_{\theta} = \frac{r}{\lambda} \frac{J_r}{\sigma} \tan \frac{\theta}{2} \quad (1)$$

where  $r$  is the radius from the burst (meters),  $\theta$  is the polar angle (degrees),  $\lambda$  is the average gamma-ray mean free path (meters),  $J_r$  is the radial Compton current source (Amps/m<sup>2</sup>) and  $\sigma$  is the air conductivity (mhos/m).

Subsequently, Grover found solutions for the quasi-static EMP with the less-limiting restriction that the radial electric fields vanish only on the earth's surface (Ref 2). This approximation is valid for an infinitely conducting earth and is a good approximation when the ground conductivity greatly exceeds the air conductivity. Grover also uses specific functional forms for the Compton current and the air conductivity. He then expands the scalar potential function in terms of Legendre polynomials and solves the resulting equations to find closed-form expressions for the electric fields.

The sources are assumed to be independent of the polar angle in both Ref 1 and 2. Furthermore, constant field-independent air chemistry and air conductivity parameters are employed throughout the solutions. The characteristics of the solutions in these two papers are summarized in Tables I and II.

TABLE I

ANALYTIC SOLUTIONS - REFERENCE 1

Assumptions	Sources/Parameters	Solutions
$E_r = 0$	$J_r = J_0 \frac{e^{-r/\lambda}}{r^2}$	$E_r = 0$
$\frac{\partial J_r}{\partial \theta} = 0$	$S = S_0 \frac{e^{-r/\lambda}}{r^2}$	$E_{\theta} = \frac{r J_r}{\lambda \sigma} \cdot \tan \frac{\theta}{2}$
$\frac{\partial \sigma}{\partial \theta} = 0$		
$J_{\theta} = 0$	$\frac{J_r}{\sigma} \propto \frac{1}{r^2}$	

TABLE II

ANALYTIC SOLUTIONS - REFERENCE 2

Assumptions	Sources/Parameters	Solution
$\frac{\partial J_r}{\partial \theta} = 0$	$J_r$ and $S$ same as Longmire	$E = -\nabla \phi$
$\frac{\partial \sigma}{\partial \theta} = 0$	$\sigma$ - Various approximate models	$\phi(r, \theta) = \sum_{\ell = \text{odd}}^{\infty} A_{\ell}(r) \cdot P_{\ell}(\cos \theta)$
$J_{\theta} = 0$		$E_r = -\frac{\partial \phi}{\partial r}$
$E_r = 0$ at $\theta = 90$ Degrees		$E_{\theta} = -\frac{1}{r} \frac{\partial \phi}{\partial \theta}$

The symbols and units in Tables I and II are defined as follows:

$E_r$  - radial electric field (Volts/m)

$E_{\theta}$  - polar electric field (Volts/m)

$J_r$  - radial Compton current (Amps/m<sup>2</sup>)

$J_{\theta}$  - polar Compton current (Amps/m<sup>2</sup>)

$S$  - ionization rate (ion pairs/m<sup>3</sup> sec)

$J_0$  - constant for a given time and yield

$S_0$  - constant for a given time and yield

$\sigma$  - air conductivity (mho/m)

\*Current address: Air Force Weapons Laboratory  
Kirtland Air Force Base  
Albuquerque, NM 87117

$\phi(r, \theta)$  - scalar potential (volts)

$A_\ell(r)$  - radial Legendre coefficients

$P_\ell(\cos\theta)$  - Legendre polynomial

Here, we present the results of an analysis extending Grover's model by eliminating the assumptions on the spatial variation of the sources. Our solution employs numerical methods that permit the use of source terms having arbitrary radial and polar variations. In addition, non-linear effects from the electric field dependence of various parameters are incorporated into the model.

In the following sections of this paper we (a) describe the numerical methods employed, (b) compare the results with those obtained in Ref 1 and 2, (c) evaluate the impact of the new effects that can be introduced with this approach, and (d) accomplish a parametric study of the quasi-static EMP considering variations in the time, yield, and water vapor content of the air.

#### NUMERICAL METHOD

For retarded times on the order of and greater than 100 microseconds after a surface nuclear burst, the time derivatives in Maxwell's equations are small compared to the other source terms, and can be set equal to zero (Ref 1). Thus,

$$\vec{\nabla} \times \vec{E} = 0 \quad (2)$$

$$\frac{1}{\mu_0} \vec{\nabla} \times \vec{B} = \sigma \vec{E} + \vec{J}_c \quad (3)$$

The electric field  $\vec{E}$  can be defined in terms of the scalar potential

$$\vec{E} = -\nabla\phi \quad (4)$$

Substitution of this into Equations (2) and (3) leads to the following equation for  $\phi$ .

$$\vec{\nabla} \cdot (\sigma \vec{\nabla}\phi) = \vec{\nabla} \cdot \vec{J}_c \quad (5)$$

Expanding Equation (5) in spherical coordinates and assuming azimuthal symmetry gives

$$\frac{1}{r^2} \frac{\partial}{\partial r} (r^2 \frac{\partial \phi}{\partial r}) + \frac{1}{r^2 \sin\theta} \frac{\partial}{\partial \theta} (\sin\theta \frac{\partial \phi}{\partial \theta}) + \frac{1}{\sigma} \frac{\partial \sigma}{\partial r} \frac{\partial \phi}{\partial r} \quad (6)$$

$$+ \frac{1}{\sigma r^2} \frac{\partial \sigma}{\partial \theta} \frac{\partial \phi}{\partial \theta} = \frac{1}{\sigma r^2} \frac{\partial}{\partial r} (r^2 J_r) + \frac{1}{\sigma r \sin\theta} \frac{\partial}{\partial \theta} (\sin\theta J_\theta)$$

This is the equation that must be solved to find the electric fields in the air.

Following Grover (Ref 2), the scalar potential is expanded in polar coordinates in the form

$$\phi(r, \theta) = \sum_{\ell=\text{odd}}^{\infty} A_\ell(r) P_\ell(x) \quad (7)$$

where the  $A_\ell(r)$ 's are unknown functions of  $r$  to be determined, and the  $P_\ell(x)$ 's are the Legendre polynomials ( $x=\cos\theta$ ). Summation over odd  $\ell$ 's satisfies the boundary conditions on the electric fields; namely, that the radial component must be zero at  $\theta = 90$  degrees for an infinite conductivity ground plane (assumed in this model), and the polar component must be zero at  $\theta = 0$  degrees because of azimuthal symmetry.

From Legendre's differential equation, it can be shown (Ref 3) that

$$\frac{1}{\sin\theta} \frac{\partial}{\partial \theta} (\sin\theta \frac{\partial P_\ell(x)}{\partial \theta}) = -\ell(\ell+1) P_\ell(x) \quad (8)$$

Substituting Equation (7) into Equation (6) and using the relationship in Equation 8, it follows that:

$$\sum P_\ell(x) \left[ \frac{2}{r} \frac{\partial}{\partial r} A_\ell(r) + \frac{\partial^2 A_\ell(x)}{\partial r^2} - \ell(\ell+1) \frac{A_\ell(r)}{r^2} \right] \quad (9)$$

$$+ \sum \frac{1}{\sigma} \frac{\partial \sigma}{\partial r} \frac{\partial A_\ell(r)}{\partial r} P_\ell(x) - \sum \frac{1}{\sigma r^2} \frac{\partial \sigma}{\partial \theta} A_\ell(r) P_\ell^1(x)$$

$$= \frac{1}{\sigma} \left[ \frac{2J_r}{r} + \frac{\partial J_r}{\partial r} + \frac{1}{r \sin\theta} \frac{\partial}{\partial \theta} (\sin\theta J_\theta) \right]$$

where  $P_\ell^1(x)$  is the first Associated Legendre polynomial. In this equation,  $\sum$  means  $\sum_{\ell=\text{odd}}^{\infty}$ .

From the orthogonality of Legendre polynomials, it is known that (Ref 3)

$$\int_0^1 P_m(x) P_n(x) dx = \frac{1}{2} \int_{-1}^{+1} P_m(x) P_n(x) dx = \begin{cases} 0 & m \neq n \\ \frac{1}{2n+1} & m = n \end{cases} \quad (10)$$

Then, multiplying both sides of Equation (9) by  $P_m(x)$  and integrating from zero to one gives (after rearrangement):

$$\left[ \frac{2}{r} \frac{\partial}{\partial r} A_m(r) + \frac{\partial^2 A_m(r)}{\partial r^2} - m(m+1) \frac{A_m(r)}{r^2} \right] \frac{1}{2m+1} \quad (11)$$

$$+ \frac{\partial A_m(r)}{\partial r} I_{A,m} - \frac{A_m(r)}{r^2} I_{B,m} = I_{C,m}$$

$$- \sum_{\substack{\ell=\text{odd} \\ \ell \neq m}} \frac{\partial A_\ell(r)}{\partial r} I_{A,\ell,m} + \sum_{\substack{\ell=\text{odd} \\ \ell \neq m}} \frac{A_\ell(r)}{r^2} I_{B,\ell,m}$$

$$IA_{l,m} = \int_0^1 \frac{1}{\sigma} \frac{\partial \sigma}{\partial r} P_l(x) P_m(x) dx \quad (12)$$

$$IB_{l,m} = \int_0^1 \frac{1}{\sigma} \frac{\partial \sigma}{\partial \theta} P_l^1(x) P_m(x) dx \quad (13)$$

and

$$IC_m = \int_0^1 \frac{1}{\sigma} \left[ \frac{2J}{r} + \frac{\partial J}{\partial r} + \frac{1}{r \sin \theta} \frac{\partial}{\partial \theta} (\sin \theta J_\theta) \right] P_m(x) dx \quad (14)$$

To solve Equation (11) an iterative scheme is used. An initial estimate of the potential is obtained by ignoring the summation terms on the right-hand side of the equation and using average, field-independent values for the electron air chemistry parameters and the electron conductivity. All the derivative terms are approximated with centered finite difference expressions on a uniform radial grid and the equation is solved using a standard algorithm for inverting the resulting tridiagonal matrix equation (Ref 4). The closed-form integrals (Equations 12-14) needed as coefficients are evaluated using Romberg integration (Ref 5).

The electric fields are then determined from the scalar potential:

$$E_r = - \frac{\partial \phi}{\partial r} = - \sum_{\ell=\text{odd}}^{\infty} \frac{\partial A_\ell(r)}{\partial r} P_\ell(x) \quad (15)$$

$$E_\theta = - \frac{\partial \phi}{\partial \theta} \frac{1}{r} = \frac{1}{r} \sum_{\ell=\text{odd}}^{\infty} A_\ell(r) P_\ell^1(x) \quad (16)$$

Using these results as a first estimate for the solution to the problem, Equation (11) is solved again; only now, the summation terms are included and the air chemistry parameters are allowed to vary according to the first estimate for the electric field. This iteration process is repeated until the fields converge to a specified tolerance at all range points and a preselected angle.

The Compton currents and ionization rates are found using analytic curve fits based on Monte Carlo calculations (Ref 6). Figure 1 gives an example of the radial current for a particular time and yield found using the fits. Shown for comparison in the figure is the approximate expression used in Ref 1 and 2 for the same physical conditions.

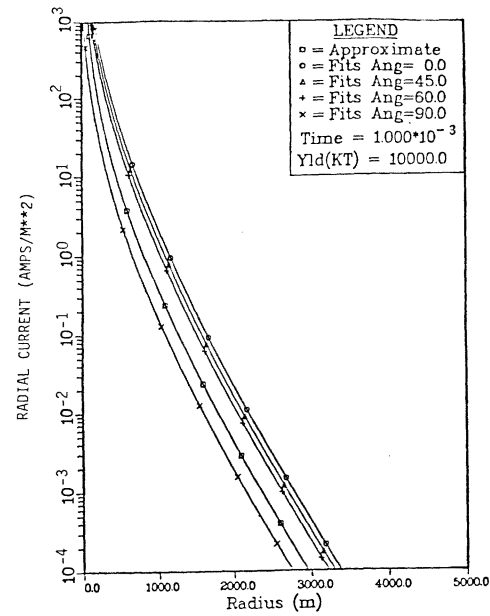


Figure 1. Radial current versus Range. Approximate form shown for Comparison

The air conductivity is solved using the standard late-time air chemistry (Ref 7). The ionic contribution is given by

$$\sigma_I = 2 \cdot e \mu_I \sqrt{\frac{S}{\gamma_I}} \quad (\text{mho/m}) \quad (17)$$

where  $\mu_I$  is the ion mobility ( $\text{m}^2/\text{V} \cdot \text{sec}$ ),  $e$  is the electron charge (coulombs),  $S$  is the local ionization rate ( $\text{i} \cdot \text{p} \cdot \text{m}^3 \cdot \text{sec}$ ), and  $\gamma_I$  is the ion-ion recombination rate ( $\text{m}^3/\text{sec}$ ). For the calculations in this work, the following were assumed:

$$\mu_I = 2.5 \times 10^{-4} \quad (\text{m}^2/\text{V} \cdot \text{sec})$$

$$\gamma_I = 2.0 \times 10^{-12} \quad (\text{m}^3/\text{sec})$$

The electron conductivity is given by

$$\sigma_e = e \mu_e \frac{S}{\alpha_e} \quad (\text{mho/m}) \quad (18)$$

where  $\mu_e$  is the electron mobility and  $\alpha_e$  is the electron attachment rate ( $\text{sec}^{-1}$ ). Variations in  $\mu_e$  and  $\alpha_e$  with electric field were included in the calculations by employing the equations developed by Longley and Longmire (Ref 8) with one modification. The mobility was constrained to a maximum value by the following equation (Ref 9).

$$\mu_{e\text{max}} = \frac{1.5}{(1.0 + 96.77 (w)^{0.789})} \quad (\text{m}^2/\text{V} \cdot \text{sec}) \quad (19)$$

## RESULTS/COMPARISONS

Using the algorithm discussed in the last section, a computer program was written to find the late-time electric fields. The test case was a ten megaton surface burst and the time of interest was  $10^{-3}$  sec (retarded time). These numbers were the same as used in a test case of Grover (Ref 2).

The radial and polar electric fields are plotted as a function of radius and polar angle in Figures 2-6. As shown in Figure 2, a sizeable radial electric field is generated. The radial field is zero at  $\theta = 90$  degrees, and above the ground plane is a rapidly decreasing function of  $r$ , changing sign at ranges beyond which the conduction current exceeds the Compton current. Also shown in Figure 2 is the analytical solution of Ref 2. The fields are slightly smaller close to the burst, and somewhat larger (negatively) at ranges beyond the crossover point.

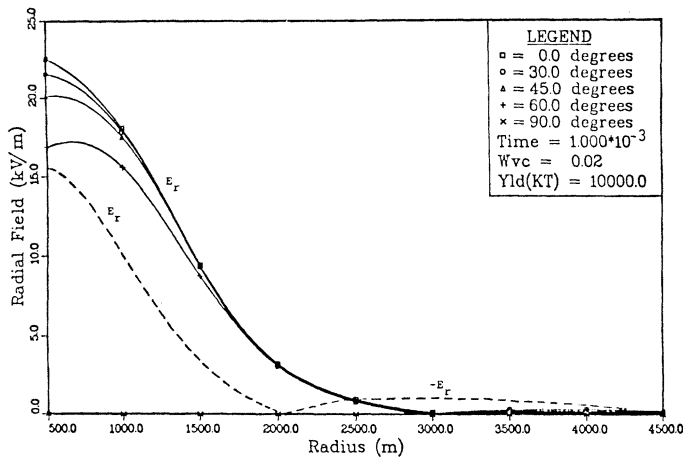


Figure 2. Radial field versus range. Ref 2 shown for comparison ( $\theta = 90$  degrees), dashed line

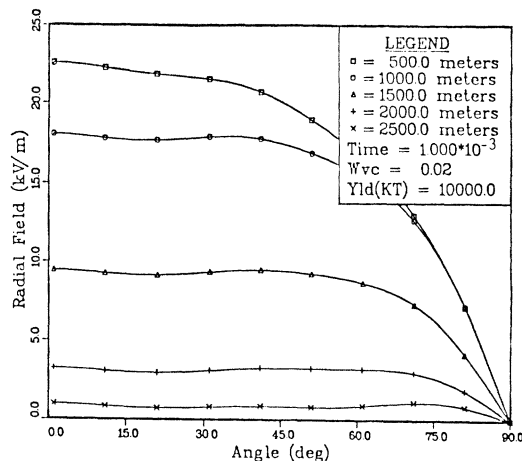


Figure 3. Radial Field Versus Angle

The polar fields are plotted in Figures 4-6. The maximum polar field is found at  $\theta = 90$  degrees, as seen in Figure 4. These results are shown in Figure 6 with the comparable polar fields from Ref 1 and 2. Our results agree closely with those of Ref 2 except for a difference in overall magnitude, which can be attributed to the non-linear effects of the air

conductivity and the angular variation of the source currents. There are significant deviations in the fields in comparison to Ref 1.

The results presented here emphasize the importance of the polar variation of the source terms, both Compton and conduction currents, in determining the EMP in the quasi-static regime. Further calculations (Ref 10) showed that variations in the electron air chemistry parameters were important in the solutions. In addition, it was determined that the theta component of the Compton current ( $J_\theta$ ) had very little effect on

the calculations. The radial field values were unaffected by the presence of ( $J_\theta$ ) and the polar fields were altered by less than five percent.

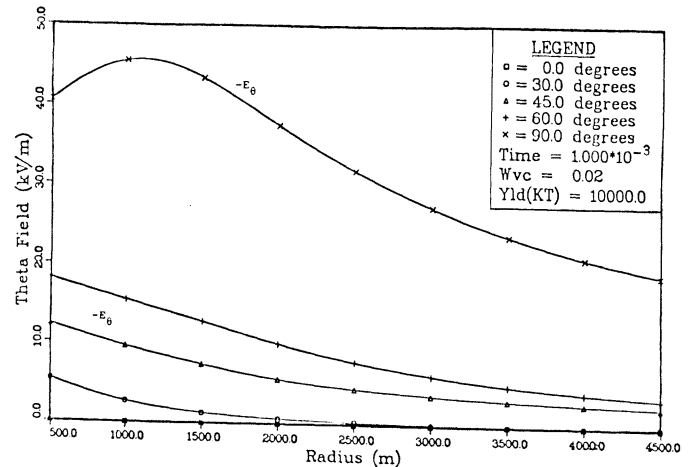


Figure 4. Polar field versus range

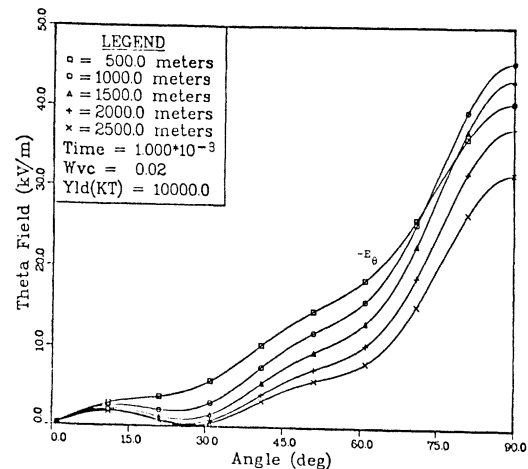


Figure 5. Polar field versus angle

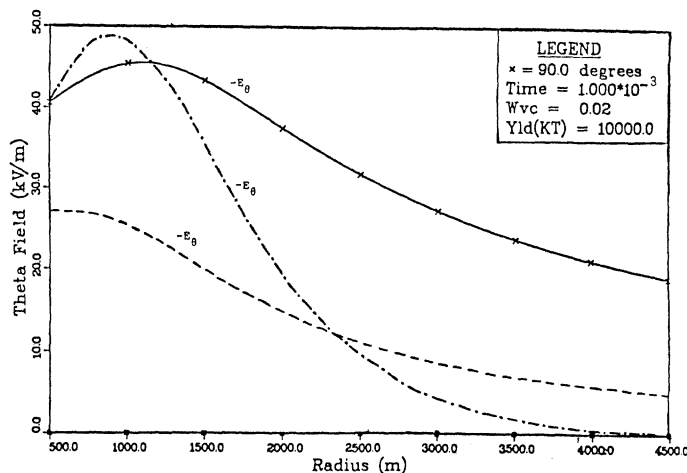


Figure 6. Polar field versus range ( $\theta = 90$  degrees). Ref 1 (dot-dash line) and Ref 2 (dashed line) shown for comparison

#### SCOPE AND LIMITATIONS

The time range of interest in this study is  $10^{-4}$  to  $10^{-1}$  sec. This range is chosen because it covers the times when either ground or air capture processes dominate the EMP sources.

The ground conductivity is assumed to be infinite. This is a fairly good approximation for later times, and smaller yields; however, the assumption is not good for points close to the burst where the air conductivity is actually larger than that of the ground.

Furthermore, no attempt has been made to incorporate self-consistent effects between the generated fields and the source currents; although, in principle, this is possible to do within the iterative procedure described.

The fundamental assumption in this problem is the quasi-static approximation which requires that the displacement current be small in comparison with the conduction current. This reduces approximately to the requirement that

$$\sigma/\epsilon \gg \frac{1}{t}$$

The approximation appears to be reasonable for the time range considered in this report.

#### PARAMETRIC STUDY

The final subject considered in this paper is a parametric study in which the effects of varying physical parameters were studied. Shown in Figure 7 is a plot of the total field versus time at five different ranges and  $\theta = 90$  degrees. Because the radial electric field is zero on the ground plane, the total field is the same as the polar component. The two plateaus appear to agree quite well with the time regimes where either ground or air capture sources dominate. Figure 8 shows the yield dependence at  $\theta = 90$  degrees. It is seen that the total field (i.e.,  $E_\theta$ ) is nearly independent of the yield at 500 meters and falls off slightly for lower yields. For larger distances the total field is more dependent on the yield. This variation can be explained by considering the ratio of  $J/\sigma$ . For short ranges this

ratio is nearly independent of yield because electrons dominate the conductivity. At greater distances the conductivity is dominated by ions and the ratio is no longer yield independent.

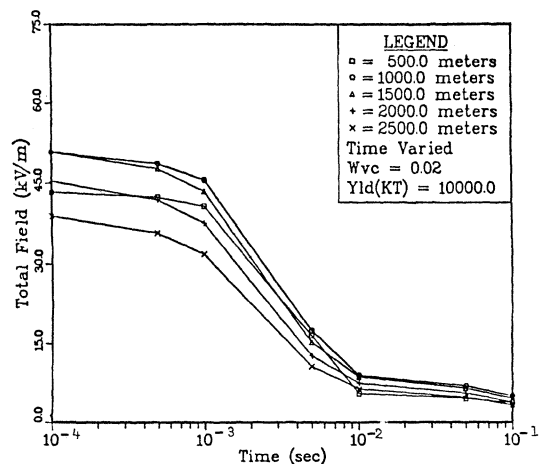


Figure 7. Total field versus time ( $\theta = 90$  degrees)

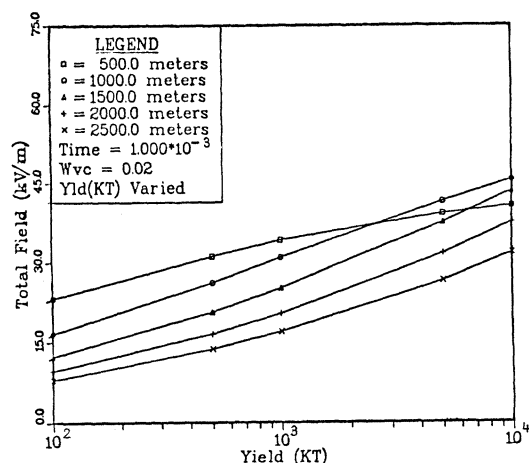


Figure 8. Total field versus yield ( $\theta = 90$  degrees)

The last parameter considered was the effect of water vapor on the total field. In Figure 9 the total field is plotted as a function of water vapor content in the air. It is obvious that the field at  $\theta = 90$  degrees varies quite substantially over the range of water vapor fractions shown. With increasing water vapor content the air conductivity decreases. Since  $E = J/\sigma$ , the field should get larger. This is clearly seen in Figure 9. Note that the dependence is greater at 500 meters because of the electron dominated conductivity.

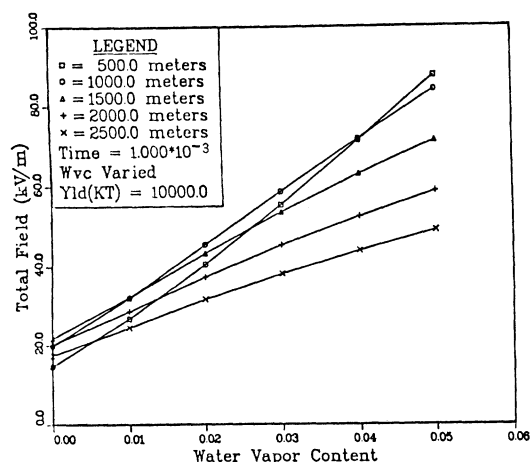


Figure 9. Total field versus water vapor content ( $\theta = 90$  degrees)

### CONCLUSIONS

The method presented in this paper provides an improved picture of the quasi-static EMP in comparison to earlier analytic models. It retains, however, the advantages of describing the surface burst EMP environment with much less computer time than needed for full time-dependent models (40-50 sec of CDC 6600 CPU time). The technique described here extends the previous work in the quasi-static regime by developing the capability to treat both spatially varying source terms and electric field dependent coefficients.

A more complete description of the numerical method can be found in Ref 10.

### ACKNOWLEDGEMENTS

The authors would like to acknowledge important contributions to this research from Gary S. Knutson.

### REFERENCES

1. Longmire, Conrad L. and James L. Gilbert. The Theory of EMP Coupling in the Source Region. MRC-R-546, Mission Research Corporation, Santa Barbara, California, February 1980, (AD-A108 751).
2. Grover, Morgan K., Some Analytic Models for Quasi-Static Source Region EMP: Application to Nuclear Lighting, RDA-TR-113202-002, R&D Associates, Marina del Rey, California, November 1980, (AD-A109 644).
3. Spiegel, Murray R., Fourier Analysis with Applications to Boundary Value Problems, New York, McGraw Hill Book Company, 1974.
4. Richtmyer, Robert D., and K. W. Morton, Difference Methods for Initial Value Problems, New York, Interscience Publishers, 1967.
5. Burden, Richard L., et al., Numerical Analysis, Boston, Prindle, Weber and Schmidt, 1978.
6. O'Dell, A. A., C. L. Longmire, and H. J. Longley, The Development of Improved Late-Time Sources for the LEMP Computer Code, MRC-R-104, Mission Research Corporation, Santa Barbara, California, November 1974, (AD-C001 246).
7. Longmire, Conrad L., "On the Electromagnetic Pulse Produced by Nuclear Explosions," IEEE Transactions on Antennas and Propagation, AP-26: 3-13, January 1978.
8. Longley, H. J. and Conrad L. Longmire, Electron Mobility and Attachment Rate in Moist Air, MRC-N-222, Mission Research Corporation, Santa Barbara, California, December 1975.
9. Smith, K. S. and W. A. Radasky, An Examination of the Behavior of the Late-Time Electronic and Ionic Conductivities Appropriate for Surface Burst EMP Calculations, DC-TN-1505-2, Dikewood Corporation, Albuquerque, New Mexico, March 1982, (AD-B064 200L), Limited.
10. Downey, James R., "The Calculation of Late-Time Surface Burst EMP Fields Using a Time-Independent Numerical Method," MS Thesis, Air Force Institute of Technology, Wright-Patterson AFB, Ohio, AFIT-GNE-83M-5, 1983.